Medicine in Novel Technology and Devices 13 (2022) 100104

Contents lists available at ScienceDirect

Medicine in Novel Technology and Devices

journal homepage: www.journals.elsevier.com/medicine-in-novel-technology-and-devices/

Full Length Article

Eularian wall film model for predicting dynamic cell culture process to evaluate scaffold design in a perfusion bioreactor

Ziyu Liu [a,b,c], Chunjing Tao [b], Shanshan Yuan [b,d], Wei Wang [e], Maryam Tamaddon [a], Liqi Ng [a], Hao Huang [b], Xiaodan Sun [c,**], Chaozong Liu [a,*]

[a] Division of Surgery & Interventional Science, University College London, Royal National Orthopaedic Hospital, Stanmore HA7 4LP, UK
[b] School of Medical Science and Engineering, Beihang University, China
[c] Key Laboratory of Advanced Materials of Ministry of Education of China, School of Materials Science and Engineering, Tsinghua University, Beijing, China
[d] Department of Cardiology, Qingdao Municipal Hospital, Shandong, China
[e] School of Science and Engineering, The Chinese University of Hong Kong, Shenzhen, China

ARTICLE INFO

Keywords:
Scaffold structure
Computational fluid dynamics
Cell attachment
Cell impinge model

ABSTRACT

In tissue engineering field, it is important to develop a suitable numerical model to evaluate scaffold geometry design. The experimental evaluation of the effect of each specific scaffold parameter on tissue regeneration requires large cost and long time expend. Dynamic cell culture is commonly used for generating tissues which could replace damaged tissues. A perfusion bioreactor model is developed which is able to simulate dynamic cell culture, to evaluate scaffold quality. The wall-film model is used to simulate cell attachment with the assumption that cells could be seen as liquid drops. In the process of cell attachment, the cells could impinge to a solid surface and form a liquid film which were considered as cell attached on the scaffold surface. Two types of cell-scaffold interactions were involved in numerical models including trap model and Stanton-Rutland (Cell impinge model—CIM) model. For trap model, all cells impinged the scaffold are seen as attached. For Stanton-Rutland model, four regimes of cell-scaffold interaction are involved in the cell attachment, including stick, rebound, spread, and splash, and only stick and spread are seen as attached. By comparison with two different numerical methods, the results showed that CIM model result is more related to the experimental results than trap model, which indicated that four regimes of cell-scaffold interaction occurred in cell attachment process. By evaluating two different geometry scaffold's cells seeding by these two models, the results further indicated that this model are able to use for assessing the scaffold design.

1. Introduction

In tissue engineering field, dynamic cell culture is commonly used for generating artifical tissues which could replace damaged tissues [1]. This process usually achieved by putting the scaffold in a purfusion bioreactor to facilitate cell growth before implantation [2]. Among all kinds of the bioreactors, perfusion bioreactor is an attractive type for researchers because it provides an oppourtunity to observe the time-dependent flow with nutreints and sometimes with alive cells and control the speed of the flow [3]. There is no doubt that the scaffold needs an adequate mechanical property and a high efficiency of the nutrient transportation. The improved structure of the scaffold (high interconnectivity) could not only enhance the nutrient transportation, but also enhance the cell and tissue growth.

In the previous studies, numerical method for investigating tissue engineering on bioreactors is mainly focus on the fluid speed and shear stress inside the scaffold [4–6]. Although cell growth and volume fractions have also been explored by CFD which Monod–Contois kinetics equation is used to predict cell growth related to shear stress [3], most of the studies are only considered 2D situation for simplifing the models. Nava et al. [7]. used Monod-Contois kinetics equation to predict tissue ingrowth in 3D model by assuming the cells as a phase of biomass. The cells, with particular non-spherical shape could be breaked up or collided each other in the flow which they should be considered in the simulation.

As the evaluation of the effect of each specific scaffold parameter on tissue regeneration requires economics-cost and time-cost experiments,

* Corresponding author.
** Corresponding author.
E-mail addresses: sunxiaodan@mail.tsinghua.edu.cn (X. Sun), chaozong.liu@ucl.ac.uk (C. Liu).

https://doi.org/10.1016/j.medntd.2021.100104
Received 18 August 2021; Received in revised form 24 November 2021; Accepted 27 November 2021

numerical models are being developed in bone tissue engineering for obtaining the optimal scaffold design for a specific application to replace the experiments.

Based on our previous numeircal study [8], it is founded that scaffold designed as high permeability, porosities and specific surface area could achieve a really high cell seeding efficiency (Truncated octahedron:60%) compared to normal cross-link scaffold design (Cubic:40%) in static cell culture system. With same macro structure size (same length, width and height) and same porosity, truncated octahedron (25.47) has a triple specific surface area than cubic scaffold structure (8.24) and it showed not only a better cell seeding efficiency but also a good cell distribution in the scaffold.

There is a common agreement made by researchers that dynamic culture could enhance cell proliferation and Guo et al. [9]. found that dynamic culture could provide a higher cell seeding efficiency than static culture [10]. However, it is also explored that static cell culture in a sufficient nutrients support bioreactor system could also achieve an increasing proliferation.

As cell distribution and cell seeding efficiency are really related to the final bioperformance, few researches have investigated on developing numerical models replacing experiments to quantify the influence factor that could enhance seeding efficiency and better uniform cell distribution. The reason is that there is still no scientific definition on how to treat cells movement and cell-material interactions in the mathematical models. Olivares et al. [11] used Eularian wall film model (trap model) followed by Euler-Lagrange approach to simulate cell seeding process assuming that only one situation occurs when a cell impinges a wall and each cell is seen as spherical and trapped by the scaffold after it touches the material surface.

In our previous study [12], we found that DPM model followed with CIM model is also one of the useful numerical models which could consider cells as discrete particles that are dispersed in the continuous phases like nutrient solution or bone marrow. In this model, the particles volume fraction should be far less than continues phase. And during this model, the particle-particle collision is neglected. In this paper, we are going to compare both numerical models (trap model and CIM model) to explore the cell seeding efficiency in a perfusion bioreactor through different scaffold geometry design with same porosity and macro size which is truncated octahedron scaffold (TO scaffold) and cross-link design (also called cubic design). Also, with same injection speed, we will further investigate how cell seeding efficiency are affected by static culture system and dynamic culture system. These two approaches include 2 different cell-material interaction scenarios which trap model defined that all cells impinged the scaffold are seen as attached and CIM model defined four regimes of cell-scaffold interaction, including stick, rebound, spread and splash. Further, after find the optimal numerical method, unit cells are analysed by the optimal method to investigate the higher cell seeding efficiency geometry and explain the reason.

2. Materials and methods

2.1. Geometry design of the scaffold

2 different structure are investigated in this paper which called cubic and truncated octahedron (TO). To compare these two scaffold structure, the macro parameters are the same with combination 7.9 mmx7.9 mm length and width at 6 mm height. Also, the porosity of 2 scaffolds are nearly the same which is 82%. The unit cell of cubic structure is a 3D structure characterized by six square faces with 6 square faces and 12 edges shown in Fig. 1 A with 1.5 mm side length, while the TO scaffold (truncated octahedron scaffold) is constructed by 8 hexagonal and 6 square faces and 36 edges shown in Fig. 1 B with macro parameter 1 mm length, width and height [8]. To compare and investigate cell seeding efficiency and other related bioperformance for these 2 structures, unit cell, 2-unit cells and models are all analysed.

2.2. Scaffold performance simulation model

2.2.1. Mesh grid of scaffold

The geometrical parameters and mesh numbers are listed in the Table 1 and physical models front views are shown in Fig. 2. The perfusion bioreactor for unit cell, 2-unit cells and scaffold are designed as a rectangular container with 11 mm, 11 mm, 28 mm length. For the whole scaffolds simulation, only quarter model is calculated by symmetric assumption and the total numbers of elements are 1116550 (Cubic design) and 1715712 (TO design). The mesh convergence has been checked from our previous work [8]. The detailed mesh of the scaffold and unit cells are shown in Fig. 3.

2.2.2. Culture medium simulation model

Cell seeding simulation model, the continuity equation controls the mass enters a system is equal to the mass leat plus the cumulation of mass in the system. The culture medium is solved by continuity equation (Eq. (1)) and Navier-Stokes equation (Eq. (2)). As the fluid phase (nutrient solution) is incompressible, the continuity equation can be simplified to a volume continuity equation:

$$\nabla \cdot \vec{u} = 0 \tag{1}$$

$$\rho\left(\frac{\partial u}{\partial t} + u \cdot \nabla u\right) = -\nabla p + p\vec{g} + \mu\nabla^2 u \tag{2}$$

Where $\vec{u}$ represents the flow velocity of nutrients flow and air, ρ is the density of the fluid (nutrients flow and air), p is the pressure and t is the time.

Volume of fluid (VOF) model—a free-surface model hich is used to track and locate the free surface. The 2 flows should be immiscible fluids that can be separated by a clear interface and are subsequently calculated by the solution of the continuity equation of the volume fraction of the

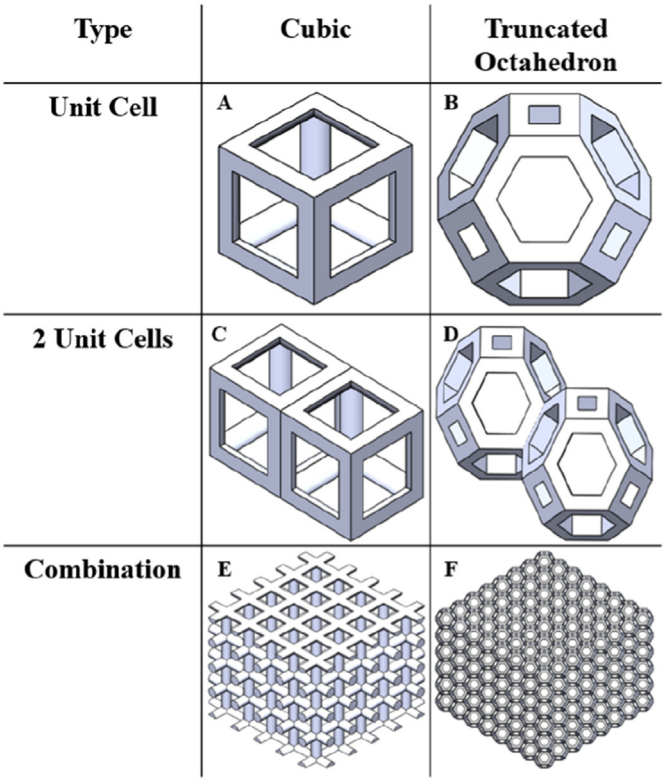

Fig. 1. Porous structures of cubic and TO scaffold.

Table 1
Mesh grid and geometrical parameters of Cubic and TO scaffold.

Type	Cubic Elements	Truncated Octahedron Elements	Cubic (Volume mm^3/Surface mm^2)	Truncated Octahedron (Volume mm^3/Surface mm^2)
Unit Cell	**714689**	**643373**	**0.66/12.02**	**0.16/4.6**
2 Unit Cells	**915125**	**642514**	**1.37/24.51**	**0.32/9.20**
Combination	**1116550**	**1715712**	**72.65/598.4**	**60.54/1541.67**

phases. In VOF model, air and nutrients solution flow motion is expressed by the Navier–Stokes equations separately.

2.2.3. Cell seeding simulation model

Cells are considered as discrete particles and they are dispersed in the continuous phases with nutrient solution or bone marrow. The cells (particle) volume fraction are far less than nutrients solution (continues phase). The cell-cell collision is neglected in this model. During the perfusion process, only scaffolds are able to absorb the secondary phase (cells) and they are all bounce back after they impinge the boundary walls of the perfusion bioreactor. All cells are seen as spherical and non-rotating, and thus the Lagrangian approach is used to trace the cells movements during cell seeding process. In this model, cell absorption was chosen Eulerian wall film model. The wall-film model allows liquid drops to impinge on a solid surface and form a liquid film. Cell attachment can be considered as the liquid film formation and captured by the wall surface in cell attachment process.

In cell culture process in dynamic perfusion reactor, the flow speed is faster and the flow is continues moving. The flowing fluid would cause interactions between the attached wall-film (cells) and fluid (nutrient solution). The conservation equations for momentum of the cells in the wall film are defined as:

$$\rho h \frac{d\overrightarrow{u_p}}{dt} = \overrightarrow{\tau_w} + \overrightarrow{F} + \overrightarrow{F_b} \tag{3}$$

Where $\overrightarrow{u_p}$ represent the cell film velocity; $\overrightarrow{\tau_w}$ represents the stress that the wall applied on the cell liquid film; $\overrightarrow{F}$ is the force per unit area that could keep the cell film on the wall's surface (scaffold beam surface); h is defined as the height at the cell location of the current cell liquid film; $\overrightarrow{F_b}$ is defined as body force term. As the cell film thickness is in a small value, the body force term could be really different because of the high acceleration rates with moving boundaries which could be expressed as:

$$\overrightarrow{\tau_w} = -2\frac{\mu_l}{h}\left(\overrightarrow{u_p} - \overrightarrow{u_w}\right) \tag{4}$$

Where μ_l is defined as viscosity of cell liquid film and $\overrightarrow{u_w}$ represents the velocity of scaffold wall which equals zero in this model as scaffolds are fixed perfectly with the perfusion bioreactor boundary walls.

Two different cell-scaffold interaction methods are provided by Stanton-Rutland model and trap model. They are all able to interact with Eulerian multiphase model by source terms of the film equations. In trap model, every cell touches the scaffold beam surface are seen as attached. Stanton-Rutland mode [13,14] contains four regimes of cell-scaffold interaction, including stick, rebound, spread, and splash. In the Eulerian multiphase interaction, secondary phase form liquid films when it is captured by wall surfaces or in other words, attached on the scaffold surface. The detail governing equations for cells are shown in our previous study [12].

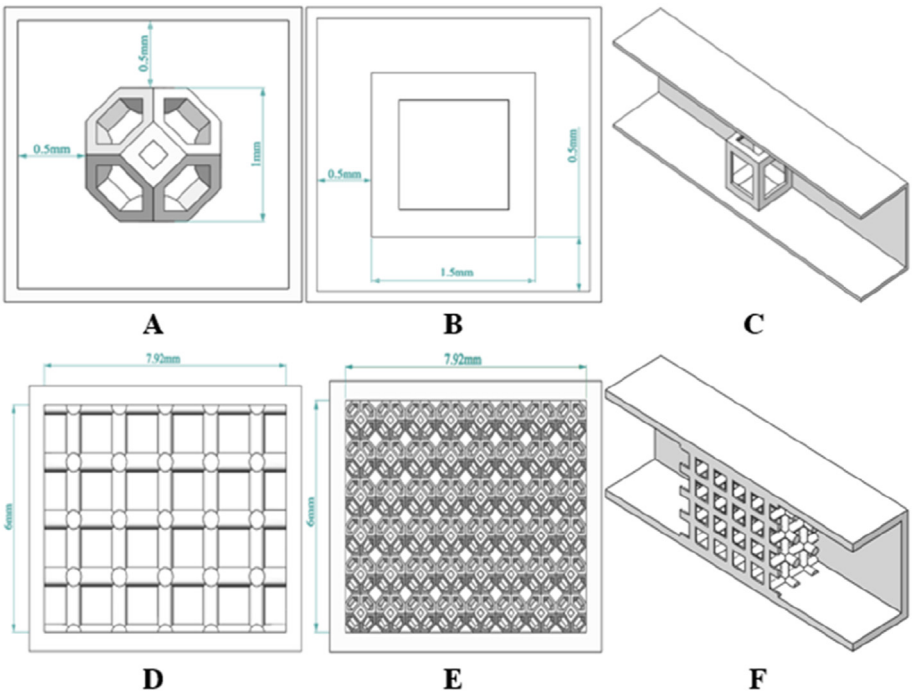

Fig. 2. Front view of the calculation system (A. TO unit cell and 2 cells in the physical domain; B. Cubic unit cell and 2 cells in the physical domain; C. Schematic diagram of physical domain for unit cells calculation; D. Cubic scaffold in the physical domain; E. TO scaffold in the physical domain; F. Schematic diagram of physical domain for scaffolds calculation).

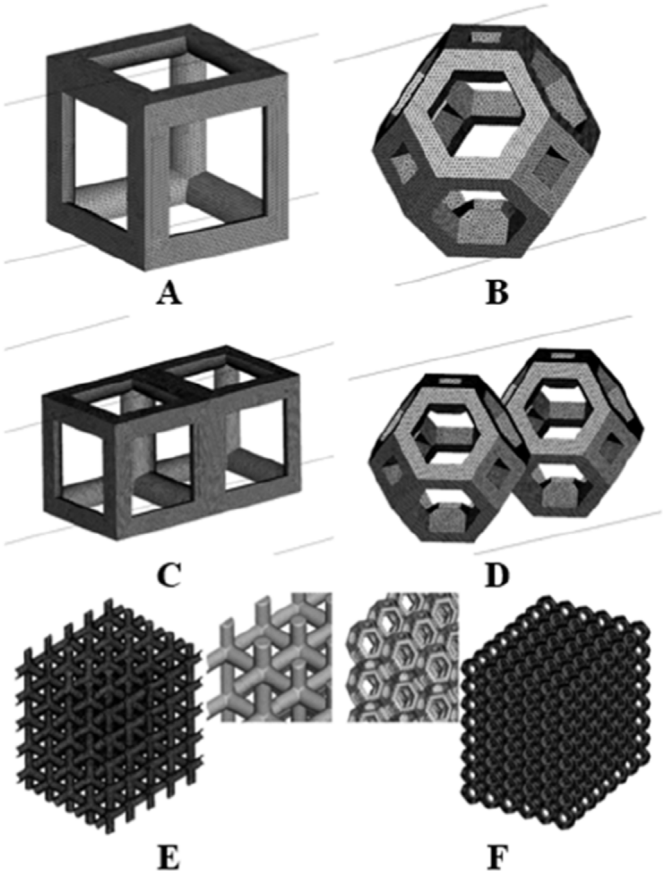

Fig. 3. Detail mesh of the scaffold (A. Cubic unit cell; B. TO unit cell; C. 2 Cubic unit cells; D. 2 TO unit cells; E. Cubic scaffold; F. TO scaffold).

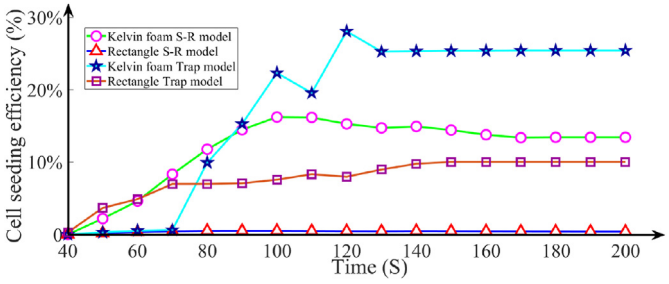

Fig. 4. Cell seeding efficiencies simulated by Stanton-Rutland model and Trap model.

2.3. Solving process and the boundary condition setup

As for the whole scaffold simulation system, the scaffold edges are seen as they are completely contacted with the bioreactor's inner surface which means that the cells could not pass the scaffold without going through the scaffold inner structure and cells are not able to attached on the scaffold edge surface which are contacted to the inner bioreactor's face. Nonslip and nonadherence conditions occurs on the wall and scaffold.

In this simulation, the fluid phase representing nutrient solution with 1.0×10^3 kg/m^3 for the density and 0.001 Pa s for the viscosity is treated as laminar and incompressible continuous fluid calculated by the continuity equation in Navier-Stokes equation. The air is also treated as laminar and incompressible continuous fluid calculated by same equation with 1.225 kg/m^3 density and 1.7894×10^{-5} Pa s viscosity. The discrete phase represented cells is calculated by tracking particles through the flow field. The particle (cell) is assumed as spherical shape which used spherical drag law to govern particle motion. Particles inject from the rectangular left hand surface flow thorugh the bioreactor and the flow flow out when they reach the outlet boundary wall (right hand surface). Side walls of the rectangular bioreactor do not trap the cells and they are reflected that all particles rebound away after they imping the wall. The inlet speed of the nutrient solution flow is 1 mm/s and the cells start injected after 20s simulation time until the nutrient solution is fullfil the perfusion bioreactor.

By Eulerian wall film model—Stanton-Rutland model, the impinge types are similar to spray droplets interaction with engine combustion internal walls. The Stanton-Rutland model, a more advance model unlike trap model, has a great advantage of predicting interactions between particles and boundary wall surface. In this impinge model, four regimes (stick, rebound, spread, and splash) are considered (O'Rourke et al., 2000). In the stick regime, the spherical particle with lower the impact energy (<16) would remain its original spherical shape and become a spherical shape film after impinge the scaffold surface. In the rebound regime, cells with higher temperature than critical transition temperature T_c and below the impact energy value (<57.7) will rebound from the scaffold surface after impinge the scaffold surface and still maintain a spherical liquid drop. In the spread regime, cells with impact energy value shoud be no less than 16 and no higher than 57.7, will form a liquid wall film after impinge the wall. In the splash regime, cells with higher than 57.7 impact energy value will separate to several smaller liquid drops when they impinge the wall. When they face, all the smaller drops are seen as dead cells. The liquid film formed on the scaffold wall surface are not seen as unstripable. Although the gravitation forces are neglected in this model, the liquid film could be striped by flow.

By Trap Model, every discrete particles (cells) imping the scaffold surface are seen as absorbed by the scaffold and added into a liquid film. In other words, it is assumed that all cells are seen as attached on the scaffold when they impinge upon the scaffold wall surface. When the cells recorded as trapped by the scaffold surface, the trajectory calculations will be terminated. Their entire mass of the cells (particles) will be instantaneously entered into the film phase (seen as attached) after they trapped. Comparing to CIM model considering impinge type of cell-scaffold based on impact energy and wall temperature, all the other governing equations of cells are same.

3. Results

3.1. Model comparison for dynamic cell seeding process

Cell seeding efficiency (Φ) is calculated as a percentage of the attached cells (Na) over the injected cells in the leat (Ni) plus attached cells and cells escaped from the outlet (Ne).

$$\Phi = \frac{N_a}{N_i + N_a + N_e} \times 100\%$$

After 140s, cells attachment is near finished on the scaffold, shown in Fig. 4.

As for Stanton-Rutland model (S-R model), the densities of cells attached on the scaffold have always a higher rate for the TO scaffold than for the cubic scaffold. it is shown that the cell seeding efficiency of TO scaffold could reach around 30% and cubic scaffold efficiency is below 10%. If we look at the cell seeding efficiency trends of TO scaffold, the efficiency increased dramatically until 80s. The graph showed that the growth slowed down noticeably after 80s until 100s. From 100s to 110s, the efficiency is relatively stable and then showed a slight decrease until 160s.

For trap model, on contrast, the cubic scaffold showed an unbelievable cell seeding efficiency which reached over 50%, and the cubic scaffold cell seeding efficiency is far higher than TO scaffold. According

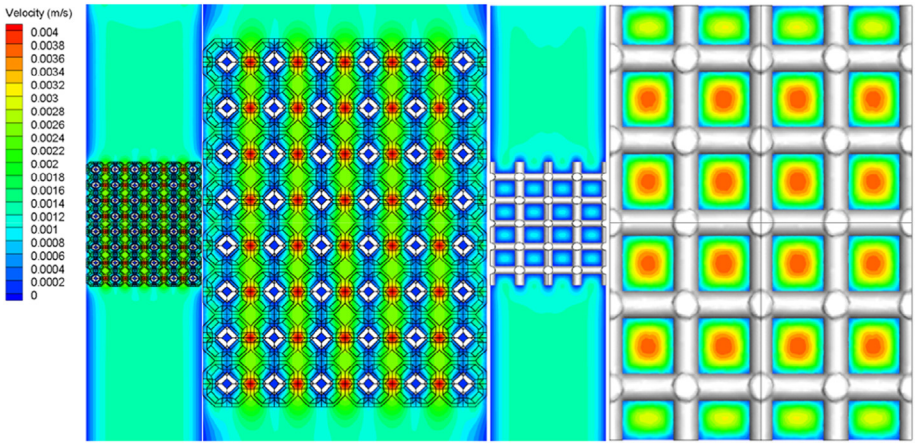

Fig. 5. Velocity flow speed (m/s) within a perfusion bioreactor of cubic and truncated octahedron scaffold.

to our previous experimental results, cubic scaffold's cell seeding efficiency with less surface area should be lower than TO scaffold. In that case, it seems that trap model is not suitable for predicting dynamic cell seeding process than S-R model.

The flow velocity counter images are shown below (Fig. 5) and it is shown that flow is highly non-uniform and the highest speed flow are occurred in the void space centre of the cubic scaffold. The lowest velocity speed is found near the cubic scaffold inner structure beam surface and the edge of the scaffold. The highest speed flow occurred at unit cells' connection area of TO scaffold and the lowest velocity happened at the centre channel of the unit cells. The pressure on the whole perfusion bioreactor channel and scaffolds are shown in Fig. 6.

To further investigate cell distribution at the inner structure of the scaffold (inner void space), we create 2 monitoring lines shown in Fig. 7. As the simulation model is quarter model and it is calculated by symmetric assumption, so the results data only contain half of the monitoring line cell distribution information. The results showed the cell distribution on the both structures. In cubic structure, the cell density reached the highest density at 0.75 mm position to the middle and the other cell density peak at 3.5 mm to the middle. Exclude the highest density on TO scaffold at the edge position, the high cell density is not in a really special

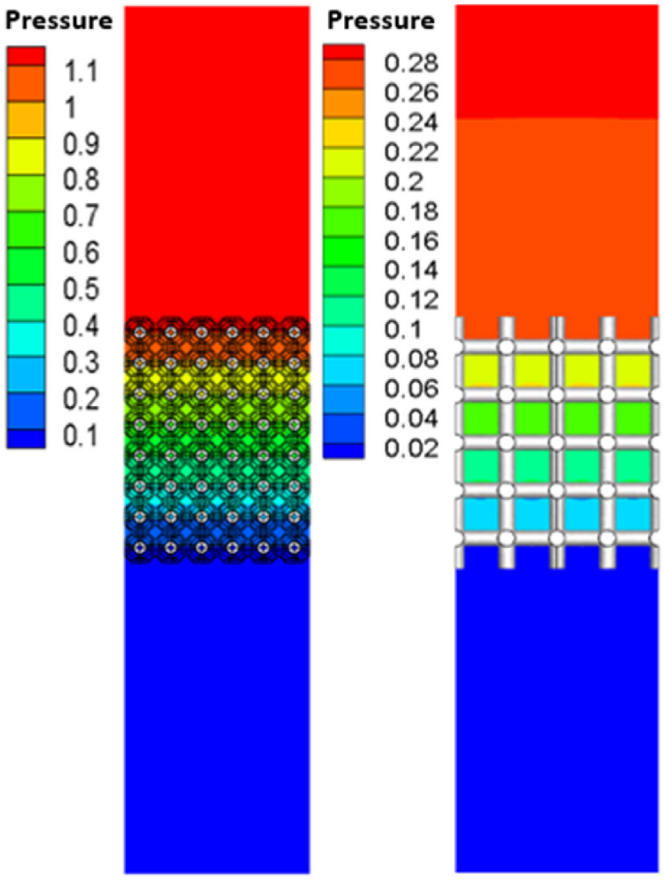

Fig. 6. Pressure (Pa) within a perfusion bioreactor of cubic and truncated octahedron scaffold.

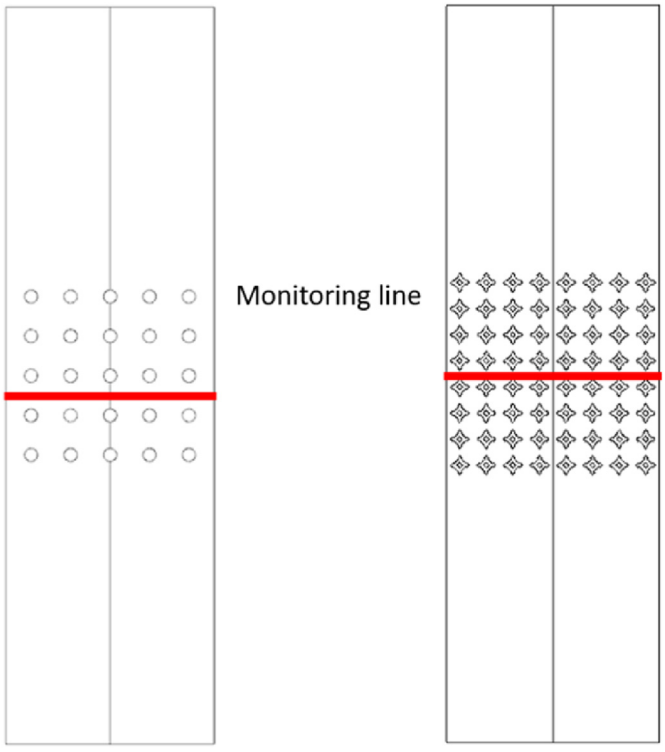

Fig. 7. Monitoring line in the perfusion bioreactor of cubic and truncated octahedron scaffold.

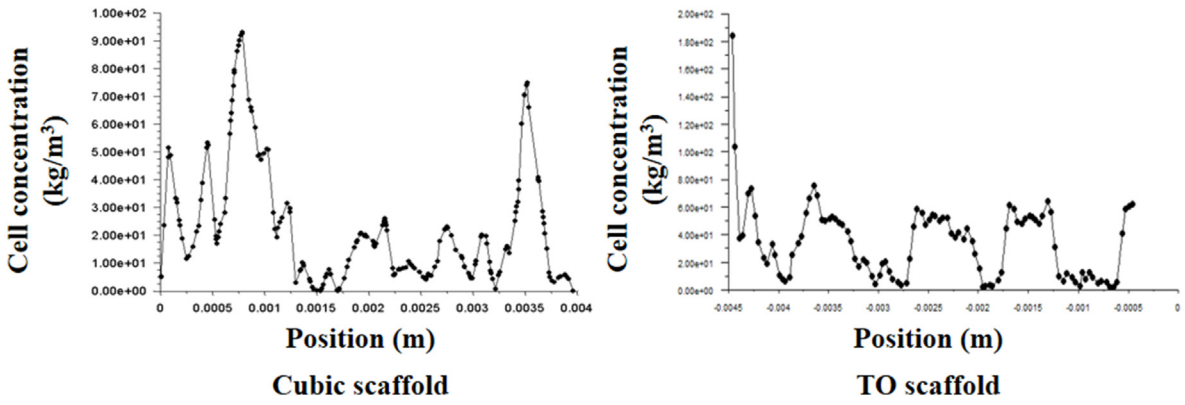

Fig. 8. Cell distribution on the monitoring line.

narrow area like cubic scaffold but there are several continuoues areas with continuoues high cell density shown in Fig. 8.

3.2. Geometry comparison for dynamic cell seeding process

After finding the optimal model which is S-R model is more accurate to simulate dynamic cell seeding process, the unit cells of 2 scaffold in perfusion bioreactors are analysed by the optimal model. The nutrient solution velocity magnitudes of unit cells are shown in Fig. 9. According to cubic structure shown in Fig. 9 A and B, the highest velocity occurred in the middle of the inner pores. As the pore size of cubic structure is 1 mm*1 mm square shape larger than TO scaffold, nutrient solution transport faster in horizontal plane than vertical plane. With smaller pores with high pore interconnectivity structure shown in Fig. 9C and D, the velocity of nutrient solution in the inner structure of TO scaffold unit cells is really low.

Cell velocity magnitudes of unit cells are shown in Fig. 10. With the same trend as nutrient solution, cells had a high speed in the inner structure than exterior of the cubic scaffold shown in Fig. 10 A and B. However, cells with lowest speed occur in the inner structure of the exterior of the TO scaffold shown in Fig. 10C and D. Compared to TO scaffold, cells that are attached on the cubic scaffold do have more opportunities to be striped by the high-speed flow. Cells are nearly suspended in the TO scaffold inner structure. In reality, this would increase cell survival probability which has been experimentally confirmed by our previous results [8]. As cubic scaffold unit cell had a higher volume and surface area than TO scaffold unit cell, there is no doubt that cubic unit cell had a higher cell attached density than TO scaffold unit cell shown in Fig. 11. More cells are attached on the exterior of the cubic scaffold but fewer cells are attached on the exterior of the TO scaffold. Another reason for TO scaffold had lower attached cell density is the distance between unit cell to the perfusion bioreactor. To make the geometrical parameters of the scaffold same, the unit cell of cubic and TO scaffold is different which cubic scaffold macro size is 1.5 mm*1.5 mm*1.5 mm and TO scaffold is 1 mm*1 mm*1 mm. The distances between perfusion bioreactor wall and scaffold were setting as 0.5 mm. The distance compare to pore size of the scaffold is smaller for cubic unit cell but larger for TO unit cell. In that case, fluid prefers to flow into the pore in cubic and it prefers to flow outside for TO scaffold which could be shown in the Fig. 12.

4. Discussion

In macroscopic scale, both truncated octahedron and cubic design have the same design parameter, but truncated octahedron scaffold

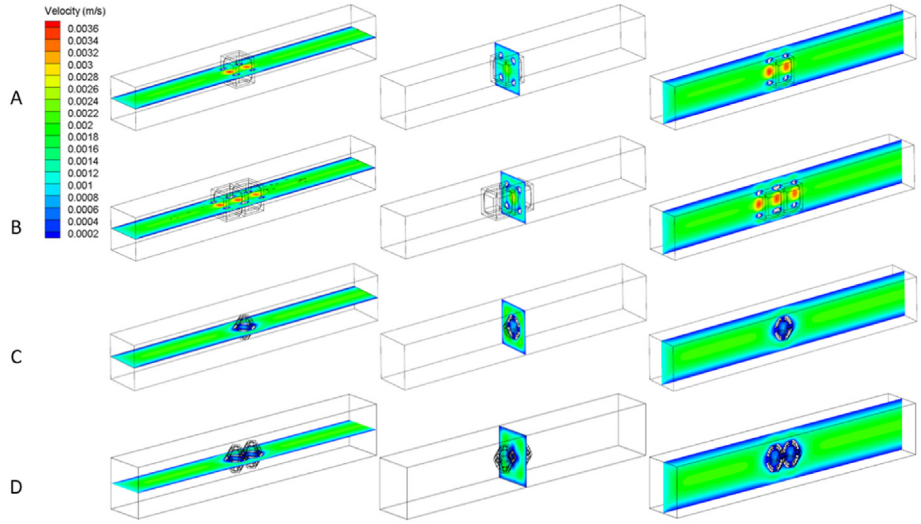

Fig. 9. Nutrient solution velocity magnitude of unit cell of scaffold (A. Cubic unit cell; B. TO unit cell; C. 2 Cubic unit cells; D. 2 TO unit cells).

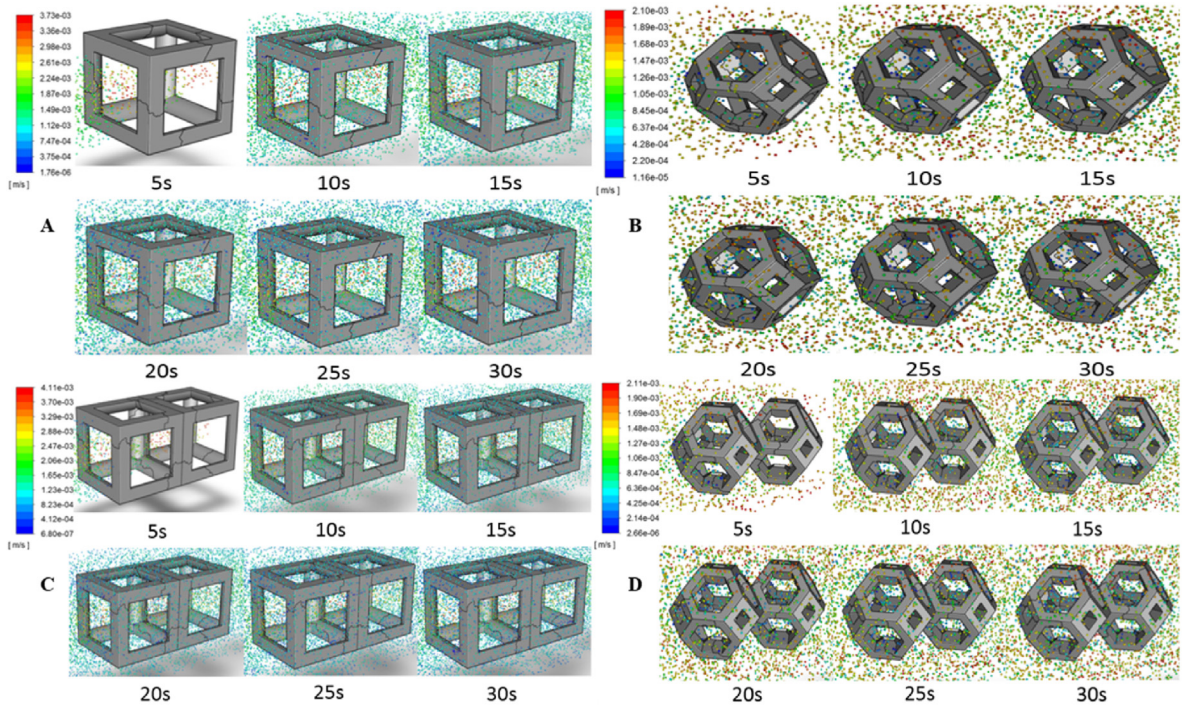

Fig. 10. Cells velocity magnitude of unit cell of scaffold (A. Cubic unit cell; B. TO unit cell; C. 2 Cubic unit cells; D. 2 TO unit cells).

design has more surface area, less material volume and higher porosity. As expected, both experimental and simulational results showed that the scaffold design has a significant effect over the cell distribution using Stanton-Rutland model which has been validated that it is good for predict cell seeding process. With nearly same material volume and macro design (same length, width and height), truncated octahedron deisgn pore size are more optimal for bone tissue. However, the simulation results shown that trap model is not suitable for simulating dynamic cell seeding process. In real dynamic culture situation, cells could be seprated by impinge the wall with high speed and some of them with really low speed and energy could not attach on the scaffold but close to the scaffold. For the first circumstance, more dead cells are included compare to the S-R model. For the other circumstance, lots of cells that are not able to attach on the scaffold but could only stay close to the scaffold surface are accounted attached in the trap model which is not suitable.

In this simulation results, it illustrated that TO scaffold with same porosity but high more surface area could get more cells attached on the scaffold in dynamic cell culture bioreator. If several thick beams with same size are arranged parallel style, the front beams near the injetion area could absorb most of the cells and the other cells would prefer to flow through void space due to the fluid mechanical theory that particles prefer to go somewhere with lower drag especially for simple structure. According to Fig. 10 A and C, nutrient solution would move fast through the pores due to the large pore size which would give cells less oppourtunities to attach on the scaffold. With same porosity and macro structure, TO scaffold' beams are connected more complicated and thinner than cubic scaffold's beams. In that case, when culture medium carried with cells flow into the TO scaffold inner structure, the drag provided by beams are more three-dimensional than cubic structure which is more like two-dimensional. The drag would force the fluid to move more slowly through the structure which provide more opportunity for cells to attach on the scaffold beam surface. Also, according to the Fig. 9C and D and Fig. 10 B and D, nutrient solution and cells had a really low speed in the interior structure of the TO scaffold. This circumstance ensure a better survival probability rate for the cells.

As the film thickness of both structures shown in Fig. 13, TO scaffold achieves a far better cell distribution than cubic scaffold in a perfusion bioreactor. During the interaction with the Eulerian wall film model, additional particles could be created when the shear stress is large enough to be stripped from the film. Mass and momentum of the particles leaving the liquid film by stripping is added to the particles (second phase) flow. Discrete particles impinging a face on a wall boundary may result in rebounding, splashing or being absorbed by the wall.

Compared to our previous study, with same inlet speed and same parameters of TO and cubic scaffolds, cell seeding efficiency in dynamic cell culture system showed a lower value than in static cell culture which TO scaffold showed a doubled seeding efficiency than static and cubic scaffold showed a 10 times more than static [8]. The reason is that the fluid is continuous flow in perfusion bioreactor which the nutrient solution carried cells flow into the system continuously but nutrient solution just injected the nutrient solution for 5s in a static cell culture well plate. In dynamic cell culture system, as the inlet flow is continuous, the average flow speed in the whole system is nearly 1 mm/s due to the physical model is an open perfusion bioreactor. However, in static cell culture system, the average flow speed is much lower though the inject speed is 1 mm/s because the physical model is a closed well plate hole. In the Eulerian wall film model, secondary phase formed liquid films are able to stripped by the flowing fluid. Lower speed of solution carrying with cells could not only ensure the survival rates of the cells because cell could break when high speed cell impinge the wall, but also could avoid the cells already attached on the scaffold to be stripped by the flow. In that case, to achieve a better cell seeding efficiency, dynamic culture flow speed should be set as lower than the injection speed of static culture.

However, even with a lower cell seeding efficiency, lots of researchers found that cell growth much faster in dynamic culture than in static culture system [9]. The reason is that dynamic culture provides much more nutrients than static culture. And nutrient transport in continuous flow is mainly depended on convection flow but in static flow is mainly depended on diffusion flow which is far slower than convection flow. Further studies are still needed to find a novel method that could enhance both cells seeding efficiency and cell growth.

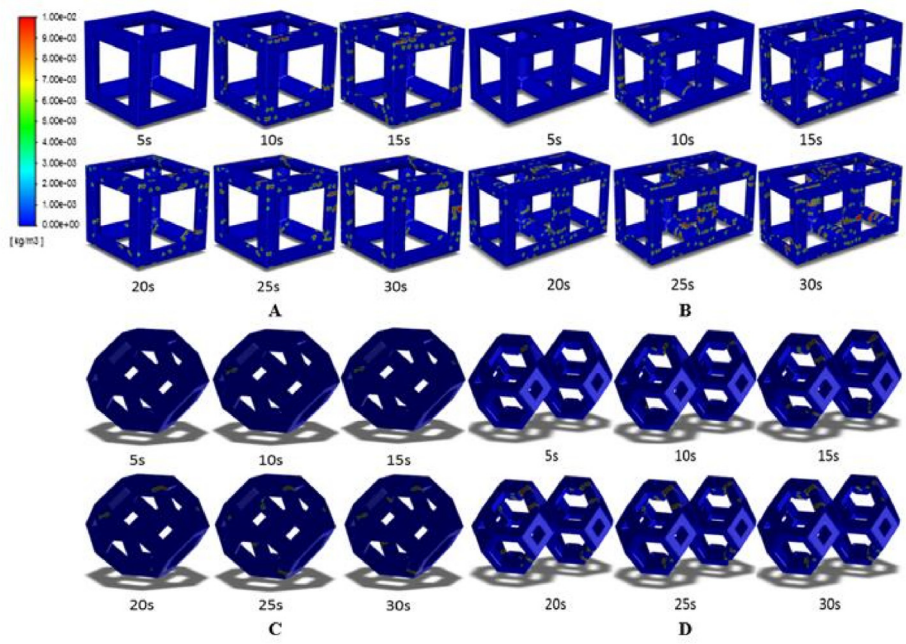

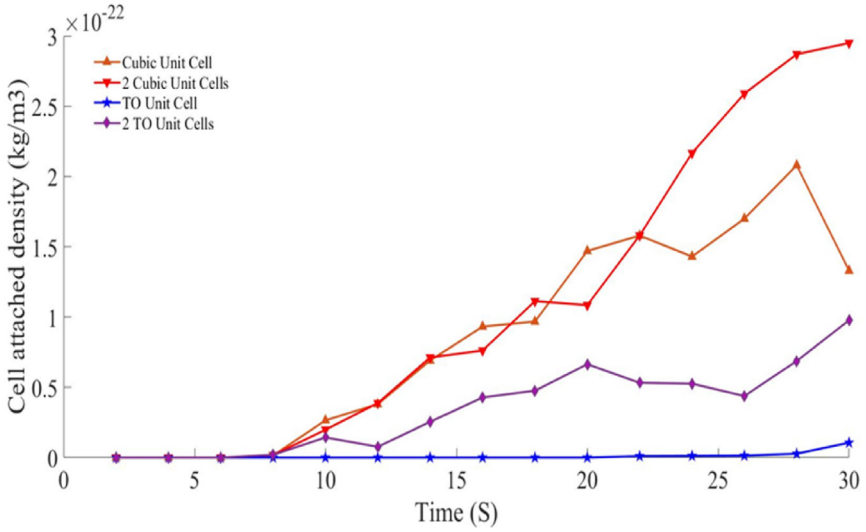

Fig. 11. Cell attachment of unit cell of scaffold (A. Cubic unit cell; B. 2 Cubic unit cells TO; C. TO unit cell; D. 2 TO unit cells; E. Density).

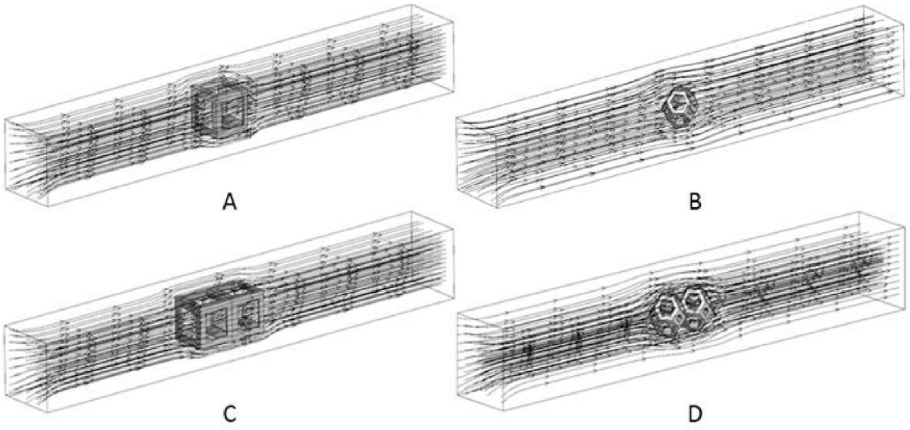

Fig. 12. Streamline of the scaffold unit cells in perfusion bioreactors (A. Cubic unit cell; B. TO unit cell; C. 2 Cubic unit cells; D. 2 TO unit cells).

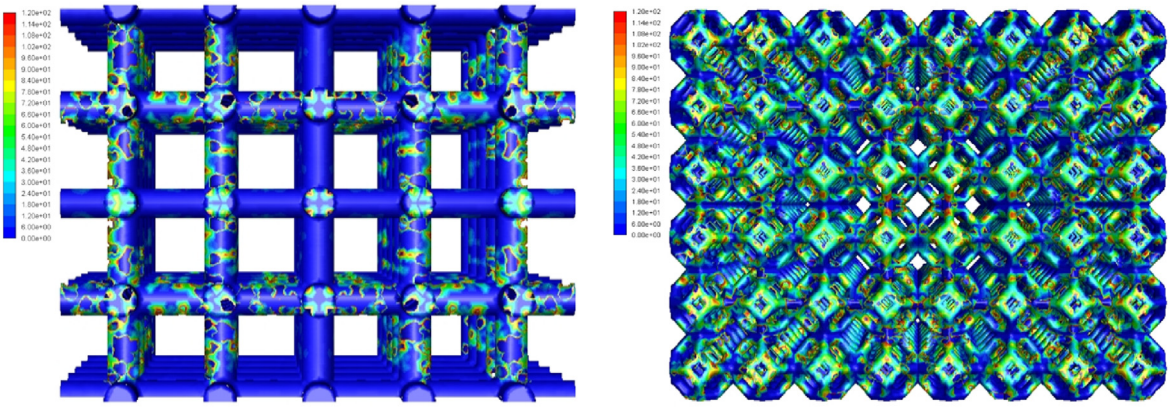

Fig. 13. Cell distribution of injected cells at 60s time by simulation.

5. Conclusion

Scaffold geometry, specific surface area, pore size and porosity are pivotal in determing optimization of the scaffold geometry parameters. The Stanton-Rutland model is appropriate to predict the cell distributions for dynamic cell seeding process. It is believe that this method improves on cell seeding models and holds the potential for more practical predictions for cell distributions in tissue engineering. It provides a more accurate impinge method to simulate cell-scaffold interaction as the position prediction can be three-dimensional. Furthermore, the simulation results showed that a polyhedron scaffold (like TO scaffold) is much more suitable for tissue engineering than normal scaffold designs. The output could also be continued to simulate cell proliferation and differention process. Therefore, this novel methodology also allows researchers to predict the initial stage of cell attachment of *in vivo* or clinical tests more accurately and may serve to reduce the numbers of experiments required during these stages. To predict more accurate results for *in vivo* or clinical experiments, loading needs to be taken in to account while simulating the cell seeding process. Chemical composition, material surface roughness and material stiffness are also influence the cell-wall interactions, and should be investigated in the future.

Funding source

This work was supported by the Versus Arthritis Research UK (Grant No: 21977), European Commission via a H2020-MSCA-RISE programme (BAMOS, Grant No: 734156), Innovative UK via Newton Fund (Grant No:102872), Engineering and Physical Science Research Council (EPSRC) via DTP CASE programme (Grant No:EP/T517793/1) and Intergovernmental cooperation in science and technology of China (No. 2016YFE0125300).

Funding source

All sources of funding should also be acknowledged and you should declare any involvement of study sponsors in the study design; collection, analysis and interpretation of data; the writing of the manuscript; the decision to submit the manuscript for publication. If the study sponsors had no such involvement, this should be stated.

Ethical approval and informed consent (if applicable)

If the work involves the use of **human subjects**, the author should ensure that the work described has been carried out in accordance with The Code of Ethics of the World Medical Association(Declaration of Helsinki) for experiments involving humans. The manuscript should be in line with the Recommendations for the Conduct, Reporting, Editing and Publication of Scholarly Work in Medical Journals and aim for the inclusion of representative human populations (sex, age and ethnicity) as per those recommendations. The terms sex and gender should be used correctly.

All **animal experiments** should comply with the ARRIVE guidelinesand should be carried out in accordance with the U.K. Animals (Scientific Procedures) Act, 1986 and associated guidelines, EU Directive 2010/63/EU for animal experiments, or the National Institutes of Health guide for the care and use of Laboratory animals (NIH Publications No. 8023, revised 1978). The sex of animals must be indicated, and where appropriate, the influence (or association) of sex on the results of the study.

The author should also clearly indicate in the Material and methods section of the manuscript that applicable guidelines, regulations and laws have been followed and required ethical approval has been obtained.

Patient consent (if applicable)

Completion of this section is mandatory for Case Reports, Clinical Pictures, and Adverse Drug Reactions. Please sign below to confirm that all necessary consents required by applicable law from any relevant patient, research participant, and/or other individual whose information is included in the article have been obtained in writing. The signed consent form(s) should be retained by the corresponding author and NOT sent to Medicine in Novel Technology and Devices.

Author contribution to study

All authors listed on your paper must have made significant contributions to the study. To ensure clarity, you are required to enter the specific details of each author's contribution, which must substantiate the inclusion of each person on the manuscript. Roles for all authors should be described using the relevant CRediT roles: Conceptualization; Data curation; Formal analysis; Funding acquisition; Investigation; Methodology; Project administration; Resources; Software; Supervision; Validation; Visualization; Roles/Writing - original draft; Writing - review & editing.

Example

Elizabeth Ash: Conceptualization, Methodology, Software. Catriona Fennell: Data curation, Writing- Original draft preparation. Linda Gruner: Visualization, Investigation. Ton Bos: Supervision. Ramya Kannan: Software, Validation. Kalaivani Moorthy: Writing- Reviewing and Editing, Supervision. Lucia Muñoz Franco: Data curation, Software,

Validation.

Please detail this information below (submit additional sheets as necessary):

Ziyu Liu: Writing, data analysis and methodology. Chunjing Tao: Data curation. Shanshan Yuan: Validation of simulation results. Wei Wang: Software use and analysis. Liqi Ng: Software use and analysis. Hao Huang:data analysis and reviewing Xiaodan Sun: Supervision, funding acquisition, writing. Chaozong Liu: Supervision, funding acquisition, writing, project administration.

Declaration of competing interest

A conflicting interest exists when professional judgment concerning a primary interest (such as patient' s welfare or the validity of research) may be influenced by a secondary interest (such as financial gain or personal rivalry). It may arise for the authors when they have financial interest that may influence their interpretation of their results or those of others. Examples of potential conflicts of interest include employment, consultancies, stock ownership, honoraria, paid expert testimony, patent applications/registrations, and grants or other funding. If there are no interests to declare then please state this: ' The authors declare that there are no conflicts of interest.'

References

[1] Wake MC, Patrick Jr CW, Mikos AG. Pore morphology effects on the fibrovascular tissue growth in porous polymer substrates. Cell Transplant 1994;3:339–43. https://doi.org/10.1177/096368979400300411.

[2] Maquet V, Jerome R. Design of macroporous biodegradable polymer scaffolds for cell transplantation. Mater Sci Forum 1997;250:15–42. https://doi.org/10.4028/www.scientific.net/MSF.250.15.

[3] Hu Y, Winn SR, Krajbich I, Hollinger JO. Porous polymer scaffolds surface-modified with arginine-glycine-aspartic acid enhance bone cell attachment and differentiation in vitro. J Biomed Mater Res Part A An Off J Soc Biomater Japanese Soc Biomater Aust Soc Biomater Korean Soc Biomater 2003;64:583–90. https://doi.org/10.1002/jbm.a.10438.

[4] Yannas IV. Tissue regeneration by use of collagen-glycosaminoglycan copolymers. Clin Mater 1992;9:179–87. https://doi.org/10.1016/0267-6605(92)90098-E.

[5] O'Brien FJ, Harley BA, Yannas IV, Gibson L. Influence of freezing rate on pore structure in freeze-dried collagen-GAG scaffolds. Biomaterials 2004;25:1077–86. https://doi.org/10.1016/S0142-9612(03)00630-6.

[6] Sanz-Herrera JA, García-Aznar JM, Doblaré M. On scaffold designing for bone regeneration: a computational multiscale approach. Acta Biomater 2009;5:219–29. https://doi.org/10.1016/j.actbio.2008.06.021.

[7] Hofmann AA, Bloebaum RD, Bachus KN. Progression of human bone ingrowth into porous-coated implants: rate of bone ingrowth in humans. Acta Orthop Scand 1997;68:161–6. https://doi.org/10.3109/17453679709004000.

[8] Liu Z, Tamaddon M, Gu Y, Yu J, Xu N, Gang F, et al. Cell seeding process experiment and simulation on three-dimensional polyhedron and cross-link design scaffolds. Front Bioeng Biotechnol 2020;8:104. https://doi.org/10.3389/fbioe.2020.00104.

[9] Bloebaum RD, Bachus KN, Momberger NG, Hofmann AA. Mineral apposition rates of human cancellous bone at the interface of porous coated implants. J Biomed Mater Res 1994;28:537–44. https://doi.org/10.1002/jbm.820280503.

[10] S F, Hulbert F, Young A, et al. Potential of ceramic materials as permanently implantable skeletal prostheses. J Biomed Mater Res 1970;4:433–56. https://doi.org/10.1002/jbm.820040309.

[11] Schliephake H, Neukam FW, Klosa D. Influence of pore dimensions on bone ingrowth into porous hydroxylapatite blocks used as bone graft substitutes. A histometric study. Int J Oral Maxillofac Surg 1991;20:53. https://doi.org/10.1016/S0901-5027(05)80698-8.

[12] Karageorgiou V, Kaplan D. Porosity of 3D biomaterial scaffolds and osteogenesis. Biomaterials 2005;26:5474–91. https://doi.org/10.1016/j.biomaterials.2005.02.002.

[13] Murphy CM, Haugh MG, O'brien FJ. The effect of mean pore size on cell attachment, proliferation and migration in collagen–glycosaminoglycan scaffolds for bone tissue engineering. Biomaterials 2010;31:461–6. https://doi.org/10.1016/j.biomaterials.2009.09.063.

[14] Blitterswijk CAV, Thomsen P, Lindahl A, Hubbell J, Williams D, Cancedda R, et al. Tissue engineering. Elsevier Academic Press; 2008. https://doi.org/10.1007/s10237-014-0606-4.